Clays and Clay Minerals, Vol. 50, No. 5, 601–613, 2002.

REFINEMENT OF THE CRYSTAL STRUCTURE OF CRONSTEDTITE-2H_2

JIŘÍ HYBLER[1,*], VÁCLAV PETŘÍČEK[1], JAN FÁBRY[1] AND SLAVOMIL ĎUROVIČ[2]

[1] Institute of Physics, Academy of Sciences of the Czech Republic, Na Slovance 2, CZ-18221 Praha 8, Czech Republic
[2] Institute of Inorganic Chemistry, Slovak Academy of Sciences, SK-84236 Bratislava, Slovakia

Abstract—The crystal structure of cronstedtite-2H_2 was refined in a hexagonal cell, space group $P6_3$, $Z = 2$, using two acicular crystals from Wheal Maudlin, Cornwall, England, and from Příbram, Czech Republic. The Wheal Maudlin sample has the chemical composition $(Fe^{2+}_{2.291}Fe^{3+}_{0.709})(Si_{1.298}Fe^{3+}_{0.707}Al_{0.004})O_5(OH)_4$ and the Příbram sample has the composition $(Fe^{2+}_{2.269}Fe^{3+}_{0.731})(Si_{1.271}Fe^{3+}_{0.724}Al_{0.005})O_5(OH)_4$. The results of refinements are as follows: $a = 5.500(1)$, $c = 14.163(2)$ Å, $V = 371.08(8)$ Å^3, $R = 3.83\%$, from 381 independent reflections, and $a = 5.4927(1)$, $c = 14.1481(2)$ Å, $V = 369.70(4)$ Å^3, $R = 4.77\%$, from 1088 independent reflections for the Wheal Maudlin and Příbram samples, respectively. The best F_o *vs.* F_c agreement was achieved when the structure was interpreted as merohedral twin; several possible twinning laws are discussed. The cronstedtite layer consists of one tetrahedral sheet and one octahedral sheet. There is one octahedral ($M1$) position, occupied by Fe only, and two tetrahedral ($T1$, $T2$) positions in the structure. Refinement of occupancy of tetrahedral sites led to values Si:Fe = 0.45:0.55(1) (Wheal Maudlin) and 0.432:0.568(8) (Příbram) in $T1$, and Si : Fe = 0.99:0.01(1) (Wheal Maudlin) and 0.888:0.112(7) (Příbram) in $T2$. Whereas the size of $T1$ is reasonable (average d_{T1-O} = 1.693 Å (Wheal Maudlin), 1.691 Å (Příbram)), $T2$ is unusually large: (d_{T2-O} = 1.740 Å (Wheal Maudlin), 1.737 Å (Příbram)) with respect to the small or almost zero Fe content. As an explanation, an alternative structure model comprising a certain amount of vacancies in $T2$ is presented. The tetrahedral rotation angle α is highly positive (+12.1° and +12.5° for the Wheal Maudlin and Příbram samples, respectively), and the layer belongs to the Franzini type A. Distortion parameters of octahedra and tetrahedra are given for both samples. One hydrogen atom engaged in the hydrogen bond was located in the Wheal Maudlin sample.

Key Words—Cronstedtite, Layer Silicate, Order-Disorder (OD), Polytypism, Twinning, X-ray Diffraction.

INTRODUCTION

Cronstedtite is an iron-bearing trioctahedral 1:1 layer silicate of the kaolin-serpentine group. The ideal composition, assuming occupancy of half of the tetrahedral sites by Fe^{3+}, is commonly reported as $(Fe^{2+}_2Fe^{3+})(SiFe^{3+})O_5(OH)_4$. Because of a deficiency of tetrahedral Fe relative to the ideal formula in most of samples studied, the general formula is often reported as $(Fe^{2+}_{3-x}\ Fe^{3+}_x)\ (Si_{2-x}Fe^{3+}_x\ )O_5(OH)_4$ (where $0 < x < 1$). Presumably, a corresponding proportion of Fe^{3+} in the octahedral sites balances the replacement of Si^{4+} by Fe^{3+} in the tetrahedral sites.

Recently, we refined structures of two polytypes: 3T, space group $P3_1$, $a = 5.497(2)$ Å, $c = 21.355(7)$ Å, $R = 5.0\%$, from Kutná Hora, Czech Republic (Smrčok *et al.*, 1994), and 1T, space group $P31m$, $a = 5.512(1)$ Å, $c = 7.106(1)$ Å, $R = 3.07\%$ from Herja, Romania, and $a = 5.503(1)$, $c = 7.104(1)$ Å, $R = 2.24\%$ from Lostwithiel, England (Hybler *et al.*, 2000). These polytypes represent OD subfamilies, or Bailey's (1969, 1988) groups A and C, respectively. Earlier studies on cronstedtite of Steadman and Nuttall (1963, 1964), Steadman (1964), Mikloš (1975), Hybler (1997, 1998), Ďurovič (1995, 1997), as well as an OD (ordered-disordered) interpretation of the structure presented by Dornberger-Schiff and Ďurovič (1975a,b) were more thoroughly referred to in these papers (Smrčok *et al.*, 1994; Hybler *et al.*, 2000).

The first structure refinement of the 2H_2 polytype was reported by Geiger *et al.* (1983). They studied a rare crystal of cronstedtite from Příbram, Czech Republic, with an unusually high Mg and Mn substitution for Fe in the octahedral sites. Because of the significant deviations from the hexagonal symmetry of the sample studied, they used a non-standard C-centered triclinic cell ($a = 5.472(8)$, $b = 9.467(19)$, $c = 14.241(39)$ Å, $\alpha = 90.015(20)$, $\beta = 90.042(18)$, $\gamma = 89.952(15)°$, $V = 737.72(28)$ Å^3, space group symbol $C1$), corresponding to a slightly deformed orthohexagonal cell. Their crystal contained multiple twins and out-of-step domains, but with a rather complicated structure model, they achieved $R = 5.4\%$ for 1832 observed reflections.

It is worth mentioning refined structures of related trioctahedral 1:1 layer silicates: lizardite-1T (Mellini, 1982; Mellini and Zanazzi, 1987; Mellini and Viti, 1994; Zhukhlistov and Zvyagin 1998), lizardite-2H_1 (Mellini and Zanazzi, 1987), Al-bearing lizardite-2H_2 (Brigatti *et al.*, 1997), amesite-2H_2, in C-centered triclinic cell (Hall and Bailey, 1979; Anderson and Bailey, 1981), amesite-2H_1 (Zheng and Bailey, 1997), non-standard triclinic polytype of amesite (Wiewióra *et al.*, 1991), lizardite-1T and 2H_1 at high temperatures (Guggenheim and Zhan, 1998). The modulated structure of greenalite

* E-mail address of corresponding author:
hybler@fzu.cz

$(Fe_3^{2+})[Si_2O_5](OH)_4$ was studied by Guggenheim and Eggleton (1998) by HRTEM and electron diffraction.

The aim of this study was to provide refined structure data for the relatively rare $2H_2$ polytype, representing the subfamily D serpentine. The stacking mode of the subfamily is characterized by $\pm b/3$ or zero shifts combined with regularly alternating 180° rotations (equivalent to alternating occupations of I and II sets of octahedral positions) of consecutive layers (Bailey 1969, 1988). In the ideal structure model of the $2H_2$ polytype, the $+b/3$ and $-b/3$ shifts alternate regularly.

SAMPLE SELECTION

Single-crystal fragments used in this study were separated from samples from Wheal Maudlin Cornwall, England and from Příbram, Czech Republic. Specimens from the former sample (British Museum No. 31146), provided by Dr R. Steadman, had been studied earlier by Steadman and Nuttall (1963, 1964). The latter sample was received from the late Prof. J. Bauer from the Institute of Chemical Technology, Prague. Both samples were also studied by Mikloš (1975). It should be pointed out that the Příbram sample is chemically quite different from the magnesian-manganoan cronstedtite from the same locality studied by Geiger *et al.* (1993).

Selected crystal fragments of the Wheal Maudlin and Příbram samples were first checked by the precession method. The *hhl* and *h0l* (hexagonal indices) photographs were recorded using unfiltered MoKα radiation, λ = 0.71073 Å to determine subfamily, polytype and to check the quality of the crystals. The procedure of subfamily and polytype determination has been described elsewhere (Ďurovič, 1997).

The Wheal Maudlin sample consisted of isolated black acicular crystals, 0.3–1 mm long, <0.1 mm thick, and almost uniform in thickness associated with several almost-parallel aggregates of acicular crystals. Their cross-section has the form of a triangle or a hexagon, sometimes rounded, irregular or even flattened. These crystals were identified as $2H_2$ polytype, in some cases partially disordered. Some other crystals, appearing in the form of truncated trigonal pyramid, were identified as a disordered polytype of the subfamily A. The microscopic check of another sample from Wheal Maudlin (Faculty of Sciences, Prague, No. 16874) revealed parallel aggregates of acicular crystals of triangular cross-section, probably of the A subfamily, with isolated acicular or cylindrical crystals of the D subfamily grown on the surface as a continuation of the A subfamily crystals. This assemblage was grown on the surface of pyrite cubes, each side measuring ~1.5 cm.

The Příbram sample contained mostly black crystals in the form of thick rods or cylinders, with rounded hexagonal or almost circular cross-sections, sometimes irregularly developed, with slightly conical terminations. Typically they are 0.3–2 mm long, 0.4–0.8 mm in diameter. Some interpenetrating intergrowths, as well as a few acicular crystals 0.5–1.5 mm long of the uniform thickness <0.1 mm, were also present. Both types of crystals were identified as $2H_2$ polytype. The $10l$ rows on $h0l$ precession photographs revealed better ordering of acicular crystals, thus one of them was chosen for data collection. Some other acicular crystals with the triangular cross-section and sharp edges were identified as partially disordered $3T$ polytype.

The partially disordered $2H_2$ polytype has also been identified in one sample from Kutná Hora, Czech Republic. However, all crystals were of cylindrical form and of quality not sufficient for data collection. The sample also contained pyramidal crystals of partially disordered $3T$ polytype.

Crystals from all samples were black in color and revealed an excellent cleavage along the basal plane. Selected crystals from Wheal Maudlin and Příbram are further referred to as WM and PB, respectively.

EXPERIMENTAL

Electron microprobe analysis

Some acicular crystals, separated from both samples, were studied by the electron microprobe analysis (EMPA). Selected crystals were checked by the precession method prior to the preparation of polished sections to be sure that the specimen really represented the $2H_2$ polytype. A preliminary check by energy dispersive spectroscopy revealed the presence of Fe, Si, O and traces of Al. Finally, several point analyses were performed on each sample and results, after averaging, are summarized in Table 1.

Check for triclinic symmetry

As the previous refinement (Geiger *et al.*, 1983) was performed with a triclinic cell, the crystals selected were checked for possible triclinic symmetry. Rotation, as well as Weissenberg, photographs of several layers perpendicular to **c** were recorded. On the rotation photographs, all symmetry-equivalent spots were perfectly fitted and no

Table 1. Electron microprobe analysis (elemental wt.%). of cronstedtite-2H_2.

Element	Wheal Maudlin Average wt.%	e.s.d.	Příbram Average wt.%	e.s.d.
Fe	52.43	0.37	52.15	0.34
Si	9.07	0.12	8.94	0.19
Al	0.03	0.05	0.04	0.05
O[1]	36.06		36.08	
H[1]	1.01		1.01	
Σ	98.60		98.22	

[1] Theoretical values of wt.% were calculated assuming 9 oxygen and 4 hydrogen atoms per formula unit.
Conditions: JEOL Superprobe 733, operating voltage 15 kV, sample current ~30 nA, standards: quartz (Si), hematite (Fe), corundum (Al), ZAF correction, average of 15 analyses.

https://doi.org/10.1346/000986002320679332 Published online by Cambridge University Press

splitting due to the lattice distortion was observed. The Weissenberg photographs (and *hk*0 precession photographs of some other crystals) revealed slight tangential splitting of diffraction spots (of the order of 0.3°). However, the angular difference of all pairs of sub-spots was uniform throughout the examined part of the reciprocal space, their intensities were equal and no radial component of shift was observed which would have signaled the cell distortion and symmetry reduction. Also, the lattice parameters refined from reflections centered by the diffractometer showed no significant deviation from the hexagonal symmetry and R_{int} was reasonable. Thus, the crystals were considered to be indeed hexagonal, and the triclinic cell used by previous authors was attributed to the different chemical composition of their sample.

Data collection

The crystals selected for data collection were mounted on the diffractometer. Crystal data, experimental details and results of refinement are summarized in Table 2. The absorption correction was performed according to the crystal shape (Templeton and Templeton, 1978) taking advantage of well-defined natural crystal faces or cleavage planes.

The structure was solved in the $P6_3$ space group. The JANA2000 (Petříček and Dušek, 2000) program package was used for the structure determination and refinement. Scattering factors were taken from *International Tables* (1974), and the starting atomic positions from the theoretical model (Bailey, 1969).

Average model

The parameters of one octahedral (*M*1), two tetrahedral (*T*1 and *T*2), and five oxygen positions, labeled according to Bailey (1969) as O1, O4, O5, OH1 and OH2 were refined. The sum of occupancy factors (Fe *vs.* Si) in tetrahedral sites was set to 1. After the introduction of anisotropic displacement factors, the *R* values converged to R = 5.61% (WM) and R = 6.12% (PB). However, calculations of distances and angles revealed the value of the angle O1–O1–O1 of basal oxygen atoms of the tetrahedral ring equal to be 119(1)° and therefore the tetrahedral rotation (ditrigonalization) angle was unexpectedly close to zero. Also, the displacement parameter of O1 was too high ($U_{eq} = 10.5 \times 10^{-2}$). The Fourier map of the tetrahedral sheet (Figure 1a) revealed elongation of the respective peaks, evidently due to superposition.

Model of merohedral twin

After unsuccessful trials to insert an extra oxygen atom, the structure was refined as a merohedral twin. The package JANA2000 enables refinement of twins composed from as many as six individuals. The twin law is expressed by the formula $[\mathbf{a}_2, \mathbf{b}_2, \mathbf{c}_2] = [\mathbf{a}_1, \mathbf{b}_1, \mathbf{c}_1] \times [\mathbf{P}_{1\rightarrow 2}]$, where $[\mathbf{a}_1, \mathbf{b}_1, \mathbf{c}_1]$ and $[\mathbf{a}_2, \mathbf{b}_2, \mathbf{c}_2]$ are the basis vectors of the first and the second twin individual respectively, and $[\mathbf{P}_{1\rightarrow 2}]$ is the twinning matrix. We used $[\mathbf{P}_{1\rightarrow 2}]$ = (0 1 0/1 0 0/0 0 1), representing the (110) twinning plane. Some other possible twinning laws and respective matrices are discussed later. This model led to R = 3.83% (WM), R = 4.77% (PB) and a more reasonable O1–O1–O1 angle of 95.8(2)° (WM) and 94.9(4)° (PB). Thus the tetrahedral rotation angle α is +12.1° (WM) and +12.5° (PB). The displacement parameter of the basal oxygen was substantially reduced (U_{eq} =3.1(3) $\times 10^{-2}$). The Fourier map of the tetrahedral sheet of one twin individual is shown in Figure 1b, as calculated for the WM sample.

Separate scale factors were set for subfamily ($h-k$ = 3n) and polytype reflections in the final phase of refinement. Their ratio converged to 1:0.93 for both specimens. In this way, the possible deficiency of intensity of polytype reflections owing to the partial stacking disorder was compensated.

Attempts to locate hydrogen atoms on the final difference Fourier map were only partially successful in the case of the WM sample. The map revealed a peak in the vicinity of OH2 (the OH group facing the interlayer space), of height 1.60 e/Å^3. The standard deviation, σ, of the peak was equal to 0.38 e/Å^3 (Ladd and Palmer, 1977). There were 14 other peaks above 3σ, but most of them

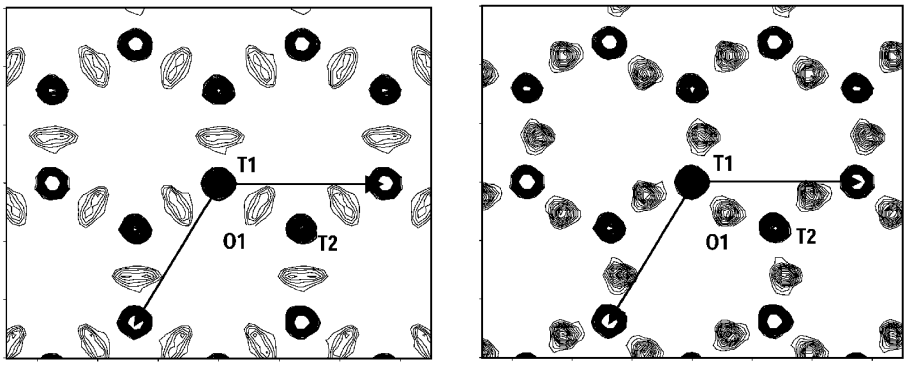

Figure 1. Electron density map of the tetrahedral sheet of cronstedtite-2H_2 from Wheal Maudlin. (a) Average model; (b) model of merohedral twin, one twin individual.

https://doi.org/10.1346/000986002320679332 Published online by Cambridge University Press

Table 2. Crystal data, experimental conditions, and refinement of cronstedtite-2H_2.

	Wheal Maudlin	Příbram
Formula	$(Fe^{2+}_{2.291}Fe^{3+}_{0.709})$	$(Fe^{2+}_{2.269}Fe^{3+}_{0.731})$
(from EMPA)	$(Si_{1.289}Fe^{3+}_{0.707}Al_{0.004})O_5(OH)_4$	$(Si_{1.271}Fe^{3+}_{0.724}Al_{0.005})O_5(OH)_4$
Crystal system	hexagonal	hexagonal
Space group	$P6_3$	$P6_3$
M_r (molecular weight)	391.63	391.83
Lattice parameters	a = 5.500(1) Å	a = 5.493(2) Å
	c = 14.163(2) Å	c = 14.148(3) Å
	V = 371.08(4) Å^3	V = 369.7(4) Å^3
Z	2	2
D_m	not measured	not measured
D_c	3.502 Mg m^{-3}	3.519 Mg m^{-3}
Radiation	MoKα graphite monochromator (0.71073 Å)	MoKα graphite monochromator (0.71073 Å)
No. of reflections for lattice parameters	38	53
θ range for lattice parameters	5.76–16.70°	7.5–23.5°
Crystal color and shape	black, acicular	black, acicular
Crystal size	0.041 × 0.042 × 0.216 mm^3	0.080 × 0.089 × 0.638 mm^3
Diffractometer	Hilger & Watts	Hilger & Watts
Collection method	ω/2θ scan, learnt profile (Clegg, 1981)	ω/2θ scan, learnt profile (Clegg, 1981)
Absorption correction	analytical (Templeton and Templeton, 1978)	analytical (Templeton and Templeton, 1978)
Absorption coefficient	7.377 mm^{-1}	7.405 mm^{-1}
T_{min}, T_{max}	0.853, 0.876	0.514, 0.611
Reflections measured, observed, independent	2185, 1413, 381	3242, 2997, 1088
θ_{max}	30°	35°
Extent of reflections measured	$-7<h<7$, $-7<k<7$, $0<l<19$	$0<h<8$, $-8<k<7$, $-22<l<22$
No. of standard reflections and interval	3/30	3/30
Variation of standard reflections	<3%	<3%
Criterion for observed	$I > 3\sigma(I)$	$I > 3\sigma(I)$
R_{int} [1]	6.51%	2.82%
R, wR, S [1] (all reflections)	3.83%, 2.58%, 2.01	4.77%, 6.31%, 3.16
No. of parameters refined	50	47
Weight	$w = 1/(\sigma^2(F_o) + (0.03\|F_o\|)^2)$	$w = 1/(\sigma^2(F_o) + (0.03\|F_o\|)^2)$
Treatment of hydrogen atoms	refined xyz of one atom	not determined
Δ/σ_{max} [1]	0.0001	0.0005
$\Delta\rho_{min}$ [1]	−3.14 eÅ^{-3}	−1.80 eÅ^{-3}
$\Delta\rho_{max}$ [1]	2.88 eÅ^{-3}	1.07 eÅ^{-3}
Ratio of twin components	0.46:0.54(1)	0.48:0.51(1)

[1] Definitions of parameters:

$$R_{int}[\%] \supset 100\frac{\sum_{n\supset 1}^{N}|F_n - \bar{F}_n|}{\sum_{n\supset 1}^{N}|F_n|} \qquad R_{int}[\%] \supset 100\frac{\sum_{h,k,l}||F_o| - |F_c||}{\sum_{h,k,l}^{N}|F_o|}$$

$$wR[\%] \supset 100\left[\frac{\sum_{h,k,l} w(|F_o| - |F_c|)^2}{\sum_{h,k,l} w|F_o|^2}\right]^{1/2} \qquad S=\left[\frac{\sum_{h,k,l} w(|F_o| - |F_c|)^2}{p-m}\right]^{1/2}$$

where N is the total number of reflections, F_n structure factor of the nth reflection, $\bar{F}_n$ average structure factor of symmetry equivalent reflections, F_o and F_c observed and calculated structure factors respectively, p number of reflections used for refinements, and m number of refined structure parameters.

Δ/σ_{max} (maximum change / estimated standard deviation) during the last refinement cycle

$\Delta\rho_{min}$ minimum residual electron density on the final difference map

$\Delta\rho_{max}$ maximum residual electron density on the final difference map

https://doi.org/10.1346/000986002320679332 Published online by Cambridge University Press

were located in the plane of basal atoms O1 and were probably produced by stacking faults. The unrefined coordinates of the atom, denoted as H2 were 0.35, 0.34 and 0.53. The refinement converged to 0.36(2), 0.36(2), 0.536(5) and the R value decreased to 3.83%. The other H1 atom near OH1 (the OH group in the center of the tetrahedral ring) was not located. The search for hydrogen atoms gave no satisfactory result for the PB sample.

The tentative reversal of the structure polarity improved further the R values to 3.61% (WM) and 4.25% (PB).

RESULTS AND DISCUSSION

The atomic coordinates and displacement parameters are listed in Table 3, and the interatomic distances and angles in Table 4. Various parameters characterizing the tetrahedral and octahedral sheets and polyhedra deformations are summarized in Table 5. Tables of observed and calculated structure factors can be obtained from the first author (J.H.) on request. Figure 2 shows the structure of cronstedtite-2H_2 (one twin individual) from the side of the tetrahedral sheet.

The Si:Fe ratio in $T1$ was refined to 0.45:0.55(1) (WM) and to 0.432:0.568(8) (PB). The refinement revealed a much smaller Fe content in $T2$; the Si:Fe ratio converged to 0.99:0.01(1) (WM) and to 0.888:0.112(7) (PB). Thus the chemical formulae, ignoring the Al content, derived from the results of the refinements are:

$(Fe^{2+}_{2.44}Fe^{3+}_{0.56})(Si_{1.44}Fe^{3+}_{0.56})O_5(OH)_4$ (WM sample)
$(Fe^{2+}_{2.32}Fe^{3+}_{0.68})(Si_{1.32}Fe^{3+}_{0.68})O_5(OH)_4$ (PB sample).

For comparison, the formulae based on the microprobe analyses are as follows:

$(Fe^{2+}_{2.291}Fe^{3+}_{0.709})(Si_{1.289}Fe^{3+}_{0.707}Al_{0.004})O_5(OH)_4$ (WM sample)
$(Fe^{2+}_{2.269}Fe^{3+}_{0.731})(Si_{1.271}Fe^{3+}_{0.724}Al_{0.005})O_5(OH)_4$ (PB sample).

The proportion of Fe^{2+} and Fe^{3+} is derived from the Si+Al content according to the general formula given in the Introduction assuming full occupancy of tetrahedral and octahedral sites.

Tetrahedral sheet

There are two tetrahedral positions, $T1$ and $T2$. Both tetrahedra are elongated (Table 4). The central atoms are displaced toward the plane of basal oxygen atom, so that the tetrahedral flattening angles are below their ideal values (Table 5). The most interesting point is that the tetrahedron $T1$ is smaller than $T2$. In the structures

Table 3a. Atomic coordinates and displacements factors, with estimated standard deviations in parentheses, of cronstedtite-2H_2 from Wheal Maudlin, Cornwall, England.

Atom	Site	x	y	z	$U_{eq}\times10^2$	$U_{11}\times10^2$	$U_{22}\times10^2$	$U_{33}\times10^2$	$U_{12}\times10^2$	$U_{13}\times10^2$	$U_{23}\times10^2$
$M1$	6c	0.3332(3)	0.0016(2)	0.4*	1.03(3)	0.76(4)	0.72(4)	1.64(2)	0.39(4)	0.07(5)	0.03(3)
$T1$[#]	2a	0	0	0.2027(2)	1.24(3)	1.25(4)	1.25(4)	1.21(5)	0.63(2)	0	0
$T2$[#]	2b	2/3	1/3	0.1997(3)	0.97(5)	0.90(6)	0.90(6)	1.09(8)	0.45(3)	0	0
O1	6c	0.3274(8)	0.1019(9)	0.1652(3)	3.1(2)	3.1(2)	3.6(3)	2.9(2)	1.9(3)	0.3(2)	0.0(2)
O4	2a	0	0	0.3258(3)	1.4(1)	1.4(2)	1.4(2)	1.5(2)	0.70(8)	0	0
O5	2b	2/3	1/3	0.3265(3)	1.7(1)	1.6(2)	1.6(2)	1.9(2)	0.80(9)	0	0
OH1	2b	1/3	2/3	0.3274(3)	1.7(1)	1.6(2)	1.6(1)	1.9(2)	0.80(8)	0	0
OH2	6c	0.333(1)	0.334(1)	0.4725(2)	1.4(2)	1.8(2)	1.2(2)	1.2(1)	0.7(2)	−0.4(2)	−0.5(3)
H2	6c	0.36(2)	0.37(2)	0.536(5)	3.6[†]						

* Fixing of origin
[#] Refined value of the occupancy ratio (Si:Fe) = 0.45 : 0.55(1) in $T1$, 0.99 : 0.01(1) in $T2$
[†] $U_{iso}\times10^2$, fixed value

Table 3b. Atomic coordinates and displacement factors, with estimated standard deviations in parentheses, of cronstedtite-2H_2 from Příbram, Czech Republic.

Atom	Site	x	y	z	$U_{eq}\times10^2$	$U_{11}\times10^2$	$U_{22}\times10^2$	$U_{33}\times10^2$	$U_{12}\times10^2$	$U_{13}\times10^2$	$U_{23}\times10^2$
$M1$	6c	0.3328(1)	0.0016(1)	0.4*	1.00(1)	1.02(2)	1.02(2)	0.97(2)	0.51(1)	0.08(2)	−0.04(1)
$T1$[#]	2a	0	0	0.2016(1)	1.16(1)	1.48(2)	1.48(2)	0.53(2)	0.74(1)	0	0
$T2$[#]	2b	2/3	1/3	0.1994(2)	1.21(2	1.54(2)	1.54(2)	0.54(3)	0.77(1)	0	0
O1	6c	0.3268(6)	0.0993(6)	0.1640(2)	3.1(1)	3.5(1)	3.5(1)	1.9(1)	1.7(1)	0.0(1)	0.02(9)
O4	2a	0	0	0.3236(2)	1.64(7)	2.03(8)	2.03(8)	0.9(1)	1.01(4)	0	0
O5	2b	2/3	1/3	0.3246(2)	1.54(7)	1.74(8)	1.74(8)	1.1(1)	0.87(4)	0	0
OH1	2b	1/3	2/3	0.3254(2)	1.56(7)	1.93(8)	1.93(8)	0.8(1)	0.96(5)	0	0
OH2	6c	0.3356(5)	0.3374(5)	0.4705(2)	1.36(7)	1.83(9)	1.58(9)	0.78(9)	0.95(6)	0.27(7)	0.24(9)

* Fixing of origin
[#] Refined value of the occupancy ratio (Si:Fe) = 0.432:0.568(8) in $T1$, 0.888:0.112(7) in $T2$
Atoms are labeled according to Bailey (1969)
$U_{eq} = 1/3(U_{11}\, a^{*2}a^2 + U_{22}b^{*2}b^2 + U_{33}c^{*2}c^2 + U_{12}a^*b^*ab\cos\gamma + U_{13}\, a^*c^*ac\cos\beta + U_{23}b^*c^*bc\cos\alpha)$

https://doi.org/10.1346/000986002320679332 Published online by Cambridge University Press

Table 4. Selected bond lengths and angles of cronstedtite-2H_2 (in Å and degrees, respectively, with estimated standard deviations in parentheses).

	Wheal Maudlin	Příbram
Octahedron:		
*M*1 –O4	2.108(3)	2.120(2)
*M*1 –O5	2.105(3)	2.120(4)
*M*1 –OH1	2.110(3)	2.122(1)
*M*1 –OH2	2.095(7)	2.091(3)
*M*1 –OH2	2.104(7)	2.077(3)
*M*1 –OH2	2.105(5)	2.089(2)
O4 –O5	3.1754(0)	3.1712(0)
O4 –OH1	3.1755(1)	3.1713(0)
O5 –OH1	3.1754(0)	3.1713(0)
O4 –OH2 × 2	2.772(6)	2.782(4)
O5 –OH2 × 2	2.764(8)	2.764(4)
OH1 –OH2 × 2	2.753(7)	2.741(4)
OH2 –OH2	3.18(1)	3.169(5)
OH2 –OH2	3.179(8)	3.169(4)
OH2 –OH2	3.172(9)	3.143(5)
O4 –*M*1 –O5	97.8(1)	96.83(8)
O4 –*M*1 –OH1	97.6(1)	96.76(8)
O5 –*M*1 –OH1	97.7(1)	96.83(7)
O4 –*M*1 –OH2	82.5(2)	82.71(9)
O4 –*M*1 –OH2	179.2(2)	178.0(1)
O4 –*M*1 –OH2	82.3(2)	82.8(1)
O5 –*M*1 –OH2	82.3(1)	82.05(8)
O5 –*M*1 –OH2	82.1(2)	82.238(9)
O5 –*M*1 –OH2	178.3(2)	177.8(1)
OH1 –*M*1 –OH2	179.8(2)	178.61(9)
OH1 –*M*1 –OH2	81.6(2)	81.5(1)
OH1 –*M*1 –OH2	81.5(2)	81.2(1)
OH2 –*M*1 –OH2	98.3(3)	99.0(1)
OH2 –*M*1 –OH2	98.4(2)	100.0(1)
OH2 –*M*1 –OH2	97.8(3)	98.0(4)
Tetrahedra:		
*T*1 –O1 × 3	1.682(4)	1.680(4)
*T*1 –O4	1.725(6)	1.726(4)
O1 –O1 × 3	2.765(5)	2.761(4)
O1 –O4 × 3	2.778(8)	2.763(4)
O1 –*T*1 –O1 × 3	110.5(3)	110.5(2)
O1 –*T*1 –O4 × 3	108.4(2)	108.4(1)
*T*2 –O1 × 3	1.722(6)	1.728(3)
*T*2 –O5	1.795(6)	1.765(4)
O1 –O1 × 3	2.860(6)	2.866(4)
O1 –O5 × 3	2.817(6)	2.804(4)
O1 –*T*2 –O1 × 3	112.3(3)	112.0(2)
O1 –*T*2 –O5 × 3	106.5(2)	106.8(1)
Other important distances and angles:		
OH2 –H2	0.91(8)	not determined
O1 –H2	1.95(9)	not determined
O1 –H2 –OH2 (hydrogen bond angle)	153(7)	not determined
Tilt of OH2 –H2 bond from vertical	11(1)	not determined
OH2 –O1 (interlayer contact)	2.791(5)	2.796(4)
O1 –O1 –O1 (tetrahedral ring angle)	95.8(2)	94.9(4)

determined so far, with the exception of cronstedtite-2H_2 (Geiger *et al.*, 1983, and this study), the larger the tetrahedron the higher the electron density at the central atom (Figure 3). Our results deviate sharply from this general trend, even more than the results of Geiger *et* al. (1983). It is of interest that both of these exceptions occur in the polytype 2H_2.

Our results, however exceptional they are, are consistent in both merohedral twin models and the average model. Table 6 lists some important parameters as calculated from structure data refined in these models.

The problem of the size of the two tetrahedra was discussed in detail by Geiger *et al.* (1983), and the reader is referred to their paper. However, we are not satisfied

https://doi.org/10.1346/000986002320679332 Published online by Cambridge University Press

Table 5. Cronstedtite-2H_2, characteristics of octahedra and tetrahedra and selected distortion parameters.

		Wheal Maudlin	Příbram
Octahedral sheet:	d_{M1-A}	2.104 Å	2.103 Å
	ψ_{M1}	60.6°	60.5°
	δ_{M1}	0.45°	0.87°
	e_{M1}	2.970 Å	2.964 Å
	e_{M1}(shared)	2.763 Å	2.762 Å
	e_{M1}(unshared)	3.176 Å	3.166 Å
	OAV_{M1}	68.9°^{2}	69.3°^{2}
	BLD_{M1}	0.158%	0.832%
	ELD_{M1}	6.957%	6.806%
	e_{M1}(unshared)/e_{M1}(shared)	1.149	1.146
Spacing between planes defined by atoms:	*M*1 and OH2	1.027 Å	0.997 Å
	*M*1 and OH1	1.028 Å	1.055 Å
	*M*1 and O4	1.051 Å	1.081 Å
	*M*1 and O5	1.041 Å	1.067 Å
	Octahedral corrugation	0.023 Å	0.025 Å
	Octahedral thickness	2.067 Å	2.065 Å
Tetrahedral sheet:	d_{T1-O}	1.693 Å	1.691 Å
	e_{T1}	2.771 Å	2.762 Å
	e_{T1} (apical)	2.778 Å	2.763 Å
	e_{T1} (basal)	2.765 Å	2.761 Å
	TAV_{T1}	1.32°^{2}	1.32°^{2}
	BLD_{T1}	0.951%	1.020%
	ELD_{T1}	0.234%	0.036%
	τ_{T1}	108.4°	108.4°
	d_{T2-O}	1.740 Å	1.737 Å
	e_{T2}	2.838 Å	2.835 Å
	e_{T2} (apical)	2.817 Å	2.804 Å
	e_{T2} (basal)	2.860 Å	2.866 Å
	TAV_{T2}	10.10°^{2}	8.12°^{2}
	BLD_{T2}	1.573%	0.797%
	ELD_{T2}	0.757%	1.093%
	τ_{T2}	106.5°	106.8°
Spacing between planes defined by atoms:	*T*1 to O1	0.531 Å	0.532 Å
	*T*2 to O1	0.489 Å	0.501 Å
	Tetrahedral thickness	2.285 Å	2.271 Å
	Δz	0 Å	0 Å
	α	+12.1°	+12.5°
Other important values:	Δ_{TM}	0.814 Å	0.823 Å
	Interlayer separation	2.729 Å	2.722 Å

d_{M-A} = mean octahedral cation–anion bond length
ψ_M = flattening angle (for an ideal, unflattened octahedron, ψ_M = 54.73°)
δ_M = counter-rotation angle, e_M = mean octahedral-edge length
d_{T-O} = mean tetrahedral cation–oxygen bond length
Δz = tetrahedral tilt, e_T = mean tetrahedral-edge length (Weiss *et al*., 1985, 1992)
α = tetrahedral rotation (ditrigonalization) angle (Radoslovich, 1961)
OAV = octahedral angle variance, TAV = tetrahedral angle variance (Robinson *et al*., 1971)
BLD = bond-length distortion, ELD = edge-length distortion (Renner and Lehmann, 1986)
e_{M1}(shared)/e_{M1}(unshared) = Ratio of mean lengths of shared and unshared edges
τ_T = tetrahedral flattening angle (for an ideal tetrahedron τ_T = 109.47°) (Robinson *et al*., 1971)
Δ_{TM} = dimensional misfit of tetrahedral and octahedral sheet (Toraya, 1981)

with any of the possibilities presented in that paper, so we have tried to find another, perhaps unconventional, explanation.

The large size of the *T*2 tetrahedron and the lower electron density at the central atom can be explained by vacancies occurring with a certain probability. The vacancies would enlarge the average size of the tetrahedron. Therefore, in sites *T*1 and *T*2, the observed electron density of the central atom can result from substitution of Si, Fe^{3+} and vacancies. The overall charge balance may be maintained by the appropriate substitution of Fe^{2+} by Fe^{3+} in the octahedral site.

https://doi.org/10.1346/000986002320679332 Published online by Cambridge University Press

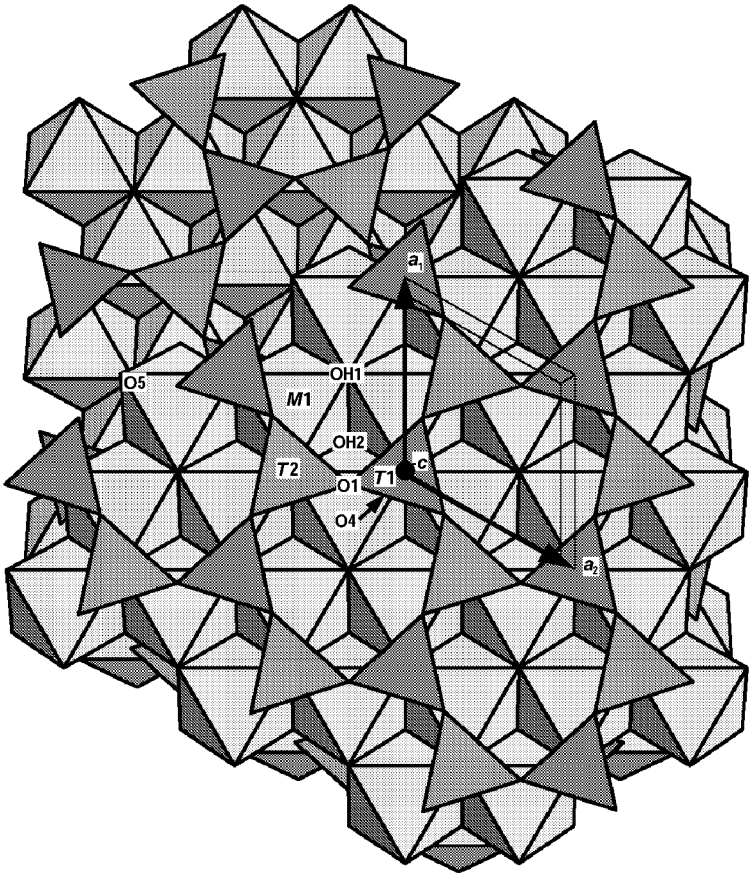

Figure 2. The structure of cronstedtite-$2H_2$, projected down [00$\bar{1}$]. Two layers are shown in a perspective view. The segment of the upper left part of the layer closer to the observer has been removed to demonstrate the stacking rule. The image was prepared using the program ATOMS (Dowty, 1991).

As the observed electron density and the size of *T*1 is almost normal (Figure 3) we suppose that *T*1 is free of vacancies. The general formula under these assumptions can then be given as:

$$(Fe^{2+}_{3-x}Fe^{3+}_{x})\ [Si_mFe^{3+}_{n}][Si_pFe^{3+}_{q}\ \square_{1-p-q}]O_5(OH)_4$$

where $x = 8 - 4m - 3n - 4p - 3q$ and $\square$ symbolizes a vacancy in *T*2. For clarity, the contents of *T*1 and *T*2 are placed in separate sets of square brackets: *T*1 first, then *T*2. This model seems to be supported by the results of EMPA indicating somewhat higher Fe content than the results of the structure refinement, assuming full occupancy of tetrahedra (see the formulae above).

However, vacancies in the tetrahedral positions of silicates are not common. They are assumed to exist, as one of a few exceptions, in the 11 Å tobermorite (Taylor, 1992) where vacancies break the 'Dreier' chain of tetrahedra into smaller segments. Thus our hypothesis has to be checked cautiously as to whether it is true or not. As the problem cannot be satisfactorily solved by a standard refinement procedure, it calls for use of some complementary method, such as the anomalous diffraction experiment. The interpretation of already recorded DAFS (diffraction anomalous fine structure) profiles of selected reflections of the PB crystal over the FeK edge using synchrotron radiation will be the subject of a separate paper.

The other possible explanation for the controversial sizes of the two tetrahedra is that this could be, in fact, an artefact caused by the presence of coherently diffracting domains of the $2H_2$ and $2H_1$ polytypes and also out-of-step domains of these in the investigated crystal. Such a coexistence has already been found by the HRTEM technique in the cronstedtite crystals from Kutná Hora (Kogure *et al.*, 2001). It drastically influences the distribution of intensities along the reciprocal rows with $h-k \neq 3n$, because these reflections for the two polytypes coincide exactly and, moreover, the proportion of such domains clearly varies from crystal to crystal. Our preliminary calculations show that this problem cannot be eliminated with two scale factors during the refinement process as for example in cronstedtite-1*T* (Hybler *et al.*, 2000), but at present we are unable to give a solution to this problem, because of its complexity. Nevertheless, the problem of the size of the tetrahedra remains open to other explanations which might emerge in future research.

https://doi.org/10.1346/000986002320679332 Published online by Cambridge University Press

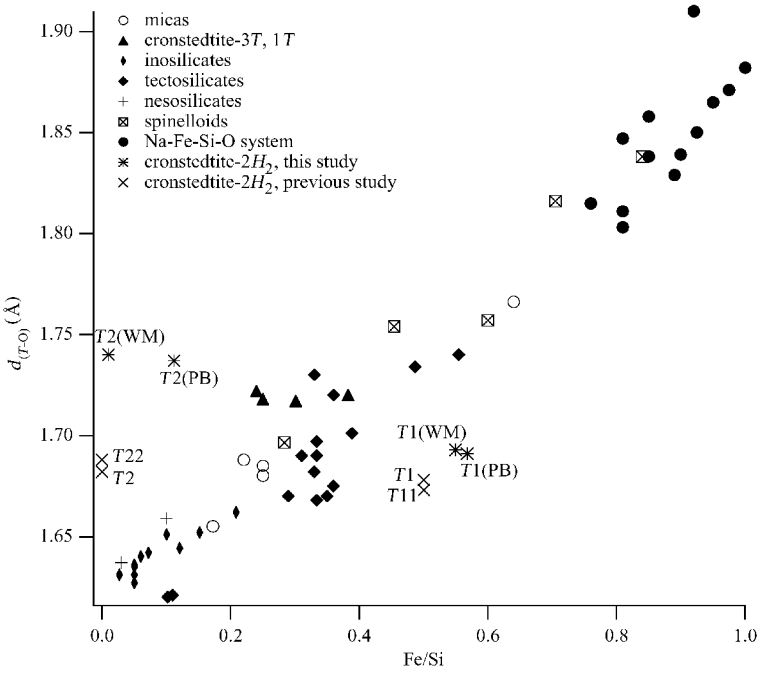

Figure 3. Dependence of the d_{T-O} on the Fe content in the tetrahedral positions of various minerals and synthetic compounds. Values from the present refinements are added for comparison. For cronstedtite-2H_2, markers are labeled in accordance with the labeling of tetrahedra in both studies. Data were obtained from the following papers: micas: ferriannite-1*M*, synthetic (Donnay *et al.*, 1964), Cs-ferriannite-1*M*, syn. (Mellini *et al.*, 1996), brittle mica anandite-2*O* (Giusepetti and Tadini, 1972), phlogopite-1*M* (Hazen *et al.*, 1981), Fe-phlogopite-1*M* (Steinfink, 1962, Semenova *et al.*, 1977); cronstedtite-3*T* and 1*T* (Smrčok *et al.*, 1994, Hybler *et al.*, 2000); cronstedtite-2H_2, previous study of Geiger *et al.* (1983); inosilicates: ferridiopside, syn. (Redhammer, 1998), aenigmatite (Canillo *et al.*, 1971); tectosilicates: K-, Rb-, Cs-leucite, syn. (Bell and Henderson, 1994), K-leucite, syn. (Palmer *et al.*, 1997), Rb-feldspar, syn. (Brunton *et al.*, 1972), K-tectosilicate (Dollase and Ross, 1993); nesosilicates: staurolite (Tagai and Joswig, 1985), yeatmanite (Kato, 1986); spinelloids, synthetic (Woodland and Angel, 1998; Angel and Woodland, 1998; Ross *et al.*, 1992); Na-Fe-Si-O system: nine synthetic solid-solutions of the composition $Na_{1-x}[Fe^{3+}_{1-x}Si_xO_2]$, where $0<x<0.2$ (Grey *et al.*, 1990).

Tetrahedral rotation (ditrigonalization). Comparison of refined structures of the polytypes of cronstedtite, lizardite and amesite confirms that the sense of rotation of tetrahedra is predominantly controlled by the OH-groups of the adjacent layer (Bailey, 1969; Mellini, 1982). The basal (bridging) oxygen atoms are moved toward the adjacent OH-groups so that the donor-to-acceptor distances of the interlayer hydrogen bonds bonding the layers together (interlayer contact) is ~2.8 Å. As a result, the tetrahedral rotation angle α of cronstedtite-1*T* is negative (Franzini's type B), and that of cronstedtite-2H_2 and 3*T* is positive (Franzini type A) (Franzini, 1969; Hybler *et al.*, 2000; Geiger *et al.*, 1983; Smrčok *et al.*, 1994). The direction of rotation in corresponding polytypes of lizardite and amesite is the same.

The absolute value of the angle α depends on the dimensional misfit of the octahedral and tetrahedral sheets. With exception of the magnesian-manganoan cronstedtite-2H_2 from Příbram ($\alpha = +10.5^\circ$), it varies within the range $11.1^\circ < \alpha < 12.5^\circ$. It is substantially larger than in lizardite (typically $1.7^\circ < \alpha < 3.5^\circ$, in the rare polytypes 2H_1 $\alpha = +6.4^\circ$, and 2H_2 $\alpha = +9.7^\circ$), but smaller than in amesite ($13.6^\circ < \alpha < 14.7^\circ$).

Octahedral sheet

The *M*1 octahedra are of almost the same size in the WM and PB structures (Table 5), and close to the values reported for other refined polytypes (Smrčok *et al.*, 1994; Hybler *et al.*, 2000) including the previous determination of the 2H_2 polytype (Geiger *et al.*, 1983). The differences in the average cation-to-anion distances are <0.01 Å. The dependence of d_{M-A} on the proportion of Fe^{3+} in octahedral positions of several divalent and trivalent iron-containing compounds is illustrated in Figure 4.

The octahedra are flattened, the octahedral flattening angles ψ_{M1}, are 60.6° and 60.5° for WM and PB, respectively. This is well within the range $\sim 58.9^\circ < \psi_M < 61^\circ$ of various serpentines. The plane of central cations is slightly closer to the plane of OH2 groups than to the plane of apical (O4 and O5) atoms. Consequently, *M*1–OH2 bonds are shorter than the other bonds in the octahedron. Also, the oxygen atom belonging to the central hydroxyl group (OH1) is closer to the plane of *M*1 atoms than the apical atoms, O5 being somewhat closer than O4. The plane defined by the OH1, O4 and O5 atoms is thus corrugated. The exact values are listed

https://doi.org/10.1346/000986002320679332 Published online by Cambridge University Press

Table 6. Selected parameters for various twin models of the structure of cronstedtite-2H_2.

Twinning matrix	Average model		Twin (0 1 0/1 0 0 /0 0 1)		Twin (0 1 0/1 0 0/0 0 −1)	
	WM	PB	WM	PB	WM	PB
R (observed)	4.56	5.92	3.02	4.59	2.86	4.17
wR (observed)	4.21	8.57	2.53	6.29	2.39	5.85
R (all)	5.66	6.12	3.83	4.77	3.66	4.35
wR (all)	4.25	8.59	2.58	6.31	2.44	5.86
S	3.31	4.29	2.10	3.16	1.98	2.93
No. of parameters refined	49	46	50	47	50	47
Vol. of the 2nd twin domain			0.54(1)	0.51(1)	0.54(1)	0.523(9)
*T*1 tetrahedron						
d_{T1-O} (in Å)	1.680	1.661	1.693	1.691	1.697	1.691
Occupancy Si:Fe (*T*1)	0.47:0.53(1)	0.43:0.57(1)	0.45:0.55(1)	0.432: 0.568(8)	0.43:0.57(1)	0.45:0.55(1)
Number of electrons	20.4	20.8	20.6	20.8	20.8	20.6
*T*1 −O1 (in Å)	1.659(5)	1.638(3)	1.682(4)	1.680(3)	1.687(6)	1.680(4)
*T*1 −O4 (in Å)	1.768(7)	1.730(5)	1.725(6)	1.726(4)	1.727(6)	1.726(4)
*T*2 tetrahedron						
d_{T2-O} (in Å)	1.716	1.713	1.740	1.737	1.739	1.737
Occupancy Si:Fe (*T*2)	1.00:0.00(1)	0.89:0.11(1)	0.99:0.01(1)	0.888: 0.112(7)	0.97:0.03(1)	0.90:0.10(1)
Number of electrons	14.0	15.3	14.1	15.3	14.4	15.2
*T*2 −O1 (in Å)	1.691(5)	1.694(3)	1.722(6)	1.728(3)	1.722(3)	1.728(4)
*T*2 −O5 (in Å)	1.791(8)	1.769(5)	1.795(6)	1.765(4)	1.789(8)	1.764(4)

Definitions of *R*, *wR* and *S* are the same as in the Table 2; *R*, *wR*, were calculated for observed and all reflections. Values d_{T1-O}, d_{T2-O} are defined in the Table 5. The number of electrons corresponds to the refined Si/Fe occupations in the *T*1 or *T*2 positions.

in Tables 4 and 5. These small, but not negligible, deviations from ideal positions mean that the octahedral sheet is polar, as in other serpentines.

The *x*, *y* atomic co-ordinates of *M*1 and OH2 are close to the ideal positions 1/3, 0 and 1/3, 1/3, respectively, required by the layer group *H*(3)1*m* of an idealized octahedral sheet. It is important to note that the symbol *H* means an alternative choice of the hexagonal cell with centering points at 1/3, 2/3, 0 and 2/3, 1/3, 0 (*International Tables for Crystallography*, 1983, p. 5).

Hydrogen bonds. The adjacent layers are linked by OH2·H2 −O1 hydrogen bonds. The OH2 −O1 interlayer donor-to-acceptor distance is given in Table 4. The WM data provided the position of the hydrogen atom H2 which is not shifted towards the acceptor atom as in the 1*T* polytype, but in an almost opposite direction. The OH2 −H2 bond is tilted by 11(1)° from vertical, and the OH2·H2 −O1 bond angle is only 153(7)°, which is substantially less than the 168(4)° in the 1*T* polytype. The interlayer separation (Table 5) is comparable with that of cronstedtite-1*T* (2.717 and 2.738 Å for two refinements) and amesite (2.71−2.74 Å), but significantly smaller than that of lizardite (~2.86 Å).

Twinning. The relatively good quality of measured crystals and the use of the structure model of merohedral twinning avoided the necessity of introducting extra atoms as in the case of Geiger's structure refinement. The twinning matrix $[\mathbf{P}_{1\rightarrow 2}]$ =(0 1 0/1 0 0/0 0 1) corresponds to the (110) twinning plane, perpendicular to the basal 001 plane. Thus the crystal can be considered as consisting of domains of both enantiomorphs of this ($2H_2$) polytype. The proportion of volumes of twin components was refined to 0.46:0.54(1) (WM) and 0.48:0.51(1) (PB). We also tested other matrices: (0 1 0/1 0 0/0 0 −1) and (−1 0 0/0 −1 0/0 0 −1). The former resulted in somewhat better *R* values (3.66% and 4.35% for WM and PB samples, respectively). The use of the latter matrix caused an increase of *R* values to 5.58% (WM) and 5.67% (PB). Also, for WM data, the volume of one twin component was refined to an unrealistic value −0.8(2). The multiple twin models comprising all possible combinations of the matrices were also tested, but the results were not convincing. The final *R* values were almost always higher, refined values of volumes of certain twin components unrealistic (below zero) and components represented by matrices (0 1 0/1 0 0/0 0 1) and (0 1 0/1 0 0/0 0 −1) strongly

https://doi.org/10.1346/000986002320679332 Published online by Cambridge University Press

correlated in the refinement. Therefore these models, as well as that represented by the matrix (−1 0 0/0 −1 0/0 0 −1) were not considered further. The R and S values, bond lengths and selected deformation parameters of tetrahedra as well as refined values of tetrahedral occupancy for the average and 'realistic' twin models are summarized in Table 6.

However, the twinning according to the law represented by the matrix (0 1 0/1 0 0/0 0 −1) would allow the existence of certain domains where the layers are turned upside down with respect to the rest of the crystal. This seems improbable, but nevertheless, cannot be completely rejected because of the almost uniform thickness and apparently non-polar character of acicular crystals of this polytype. The domain boundary might be created by an accidental interstratification of the 2:1 layer, brucite sheet or a group of chlorite packets into the cronstedtite structure. However, the actual HRTEM studies performed by Kogure (pers. comm.) have not yet revealed any sign of reversals of layer polarity in the crystals of the subfamily D. Appearance of layers other than 1:1 in cronstedtite is very rare; only one case of a chlorite packet was mentioned by Kogure *et al.* (2001)

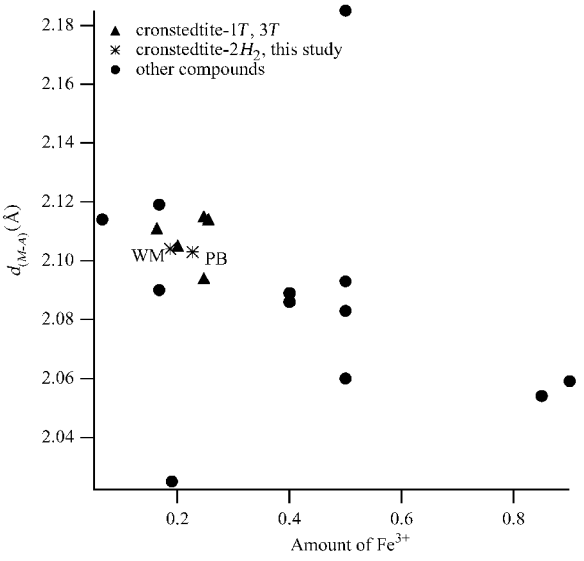

Figure 4. Dependence of the d_{M-A} on the amount of Fe^{3+} in octahedral positions. Data for Fe^{2+} and Fe^{3+} in octahedra of various minerals and synthetic compounds were plotted: cronstedtite-3T and 1T (Smrčok *et al.*, 1994; Hybler *et al.*, 2000), $Fe_4Ge_2O_9$ (Modaressi *et al.*, 1984), alluadite, syn. (Yakubovich *et al.*, 1977), $SrZn_{2/3}Mn_{4/3}Fe_{16}O_{27}$ (Collomb *et al.*, 1989), jugoldite (Allmann and Donnay, 1973), magnetite (de Boer *et al.*, 1950; Wechsler *et al.*, 1984; Della Giusta *et al.*, 1987), fluorriebeckite (Hawthorne, 1978), hexagonal Ca-ferrite (Arakheeva and Karpinskii, 1987), voltaite (Mereiter, 1978), and hulsite (Konnert *et al.*, 1976). The amount of Fe^{3+} for the present study assumes full occupancy of tetrahedra. The study of cronstedtite-2H_2 of Geiger *et al.* (1983) is not included in the graph, because of the substantial Mg and Mn contents in the octahedra.

within a rare cronstedtite crystal with intergrown domains of subfamilies A and C. Crystals belonging to subfamilies other than D are distinctly polar (pyramidal or conical), so the possiblity of this kind of twinning seems to be improbable.

Polytypism and morphology

Recent studies of cronstedtite polytypes revealed some characteristic features concerning their occurrence, morphology and properties.

Firstly, some of the standard (maximum degree of order, MDO) polytypes occur more frequently than the others of the same subfamily. These polytypes are: 3T, 1T and 2H_2 in subfamilies A, C and D, respectively. In addition, the majority of samples found in nature are the 1T polytype, followed by less common 3T, and relatively rare 2H_2 polytypes. Other polytypes, even the standard ones are much more rare and usually they are found as intergrowths with some of the 'preferred' ones, such as 1M with the 3T polytype (Ďurovič, 1997), or 2H_1 with the 2H_2 polytype (Kogure *et al.*, 2001).

Secondly, the symmetry of a polytype is usually reflected by the morphology of crystals: cones or trigonally deformed cones are typical of 1T , trigonal pyramids, plates and needles are typical of 3T, and less typical of 1T. Acicular or columnar crystals with hexagonal or rounded trigonal cross-section are typical for 2H_2. However, the degree of ordering can vary, even within one crystal individual. Therefore, these findings can be generalized to disordered polytypes of their respective subfamilies.

Thirdly, the 2H_2 polytype often appears together with 3T, but usually as isolated crystals, not as oriented intergrowths; this coexistence was found in material from Wheal Maudlin, Příbram as well as from Kutná Hora. Usually the isolated 2H_2 crystals grow on aggregates of 3T as a substrate. The opposite is not true; 3T is not always accompanied by 2H_2 polytype. No polytype of the subfamily B has been found to date, supporting the second rule of Steadmann (1964), which excludes the combination of $\pm a_i/3$ shifts with $(2n+1) \times 60^\circ$ rotations of 1:1 layers.

ACKNOWLEDGMENTS

This study was supported by grants 202/00/0645 and 203/99/0067 from the Grant agency of the Czech Republic and by grant 1/4088/98 from the Grant agency of the Slovak Academy of Sciences. We thank V. Cílek and especially Ms I. Konopáčová from the Geological Institute of the Academy of Sciences of the Czech Republic for preparing the polished sections. The electron microprobe analysis was performed with the aid of the late M. Šimečková. We thank the late Prof. J. Bauer, Institute of Chemical Technology Prague, R. Steadmann, University of Bradford, UK, and K. Melka, Geological Institute of the Academy of Sciences of the Czech Republic, Prague and Faculty of Sciences, Charles University, Prague for providing samples. The figures were prepared with the help of P. Machek and M. Dušek. Critical comments by M.

Mellini, of the University of Sienna, Italy, and valuable suggestions by a second, anonymous referee helped us to improve the manuscript.

REFERENCES

Allmann, R. and Donnay, G. (1973) The crystal structure of jugoldite. *Mineralogical Magazine*, **39**, 271–281.

Anderson, C.S. and Bailey, S.W. (1981) A new cation ordering pattern in amesite-2H_2 *American Mineralogist,* **66**, 185–195.

Angel, R.J. and Woodland, A.B. (1998) Crystal structure of spinelloid II in the system Fe_3O_4-Fe_2SiO_4. *European Journal of Mineralogy,* **10**, 607–611.

Arakheeva, A.V. and Karpinskii, O.G. (1987) Crystal structure of the ternary hexagonal Ca ferrite $Ca_{3.0}Fe_{14.82}O_{25}$. *Kristallografiya*, **32**, 59–61 (in Russian).

Bailey, S.W. (1969) Polytypism of trioctahedral 1:1 layer silicates. *Clays and Clay Minerals*, **17**, 355–371.

Bailey, S.W. (1988) Polytypism of 1:1 layer silicates. Pp. 9–27 in: *Hydrous Phyllosilicates (Exclusive of Micas)* (S.W. Bailey, editor). Reviews in Mineralogy, **19**, Mineralogical society of America, Washington, D.C.

Bell, A.M.T. and Henderson, C.M.B. (1994) Rietveld refinement of the structures of dry-synthesized $M$$Fe^{III}Si_2O_6$ leucites (M=K,Rb,Cs) by synchrotron X-ray powder diffraction. *Acta Crystallographica,* **C50**, 1531–1536.

Brigatti, M.F., Galli, E., Medici, L. and Poppi, L. (1997) Crystal structure of aluminian lizardite-2H_2. *American Mineralogist,* **82**, 931–935.

Brunton, G.D., Harris, L.A. and Kopp, O.C. (1972) Crystal structure of rubidium-iron feldspar. *American Mineralogist*, **57**, 1720–1728.

Canillo, E., Mazzi, F., Fang, J.H., Robinson, P.D. and Ohya, Y. (1971) The crystal structure of aenigmatite. *American Mineralogist*, **56**, 427–445.

Clegg, W. (1981) Faster data collection without loss of precision. An extension of the learnt profile method. *Acta Crystallographica,* **A37**, 22–28.

Collomb, A., Litsardakis, G., Samaras, D. and Pannetier, J. (1989) Neutron diffraction studies of the crystallographic and magnetic structures of $SrZn_{2/3}Mn_{4/3}Fe_{16}O_{27}$. *Journal of Magnetism and Magnetic Materials*, **78**, 219–225.

de Boer, V., van Santen, J.H. and Verwey, E.J.W. (1950) The electrostatic contribution to the lattice energy of some ordered spinels. *Journal of Chemical Physics*, **18**, 1032–1034.

Della Giusta, A., Princivalle, F. and Carbonin, S. (1987) Crystal structure and cation distribution in some natural magnetites. *Mineralogy and Petrology*, **37**, 315–321.

Dollase, W.A. and Ross, C.R., II (1993) Crystal structure of the body centered tetragonal tectosilicates. *American Mineralogist*, **78**, 627–632.

Donnay, G., Morimoto, N., Takeda, H. and Donnay, J.H.D. (1964) Trioctahedral one-layer micas. I. Crystal structure of a synthetic iron mica. *Acta Crystallographica*, **17**, 1369–1373.

Dornberger-Schiff, K. and Ďurovič, S. (1975a) OD-interpretation of kaolinite-type structures - I: Symmetry of kaolinite packets and their stacking possibilities. *Clays and Clay Minerals*, **23**, 219–229.

Dornberger-Schiff, K. and Ďurovič, S. (1975b) OD-interpretation of kaolinite-type structures - II: The regular polytypes (MDO-polytypes) and their derivation. *Clays and Clay Minerals*, **23**, 231–246.

Dowty, E. (1991) *ATOMS, a computer program for displaying structures.* Shape Software, Kingsport, Tennessee.

Ďurovič, S. (1995) Troubles with cronstedtite-1*M*. *Geologica Carpathica - Clays*, **4**, 88.

Ďurovič, S. (1997) Cronstedtite-1*M* and coexistence of 1*M* and 3*T* polytypes. *Ceramics-Silikáty*, **41**, 98–104.

Franzini, M. (1969) The A and B mica layers and the crystal structure of sheet silicates. *Contributions to Mineralogy and Petrology,* **21**, 203–224.

Geiger, C.A., Henry, D.L., Bailey, S.W. and Maj, J.J. (1983) Crystal structure of cronstedtite-2H_2. *Clays and Clay Minerals*, **31**, 97–108.

Giusepetti, G. and Tadini, C. (1972) The crystal structure of the 2*O* brittle mica anandite. *Tschermaks Mineralogische und Petrographische Mitteilungen*, **18**, 169–184.

Grey, I.E., Hoskins, B.F. and Madsen, I.C. (1990) A structural study of the incorporation of silica into sodium ferrites, $Na_{1-x}[Fe^{3+}_{1-x}Si_xO_2]$, x = 0 to 0.20. *Journal of Solid State Chemistry*, **85**, 202–219.

Guggenheim, S. and Eggleton, R.A. (1998) Modulated crystal structures of greenalite and caryopilite: A system with long-range, in-plane structural disorder in the tetrahedra sheet. *The Canadian Mineralogist*, **36**, 163–179.

Guggenheim, S. and Zhan, W. (1998) Effect of temperature on the structures of lizardite-1*T* and lizardite-2H_1. *The Canadian Mineralogist*, **36**, 1587–1594.

Hall, S.H. and Bailey, S.W. (1979) Cation ordering pattern in amesite. *Clays and Clay Minerals*, **27**, 241–247.

Hawthorne, F.C. (1978) The crystal chemistry of the amphiboles. VIII. The crystal structure and site chemistry of fluor-riebeckite. *The Canadian Mineralogist*, **16**, 187–194.

Hazen, R.M., Finger, L.W. and Velde, D. (1981) Crystal structure of a silica- and alkali-rich trioctahedral mica. *American Mineralogist*, **66**, 586–591.

Hybler, J. (1997) Determination of crystal structures of minerals affected by twinning. PhD thesis, Charles University, Prague, Czech Republic, 138 pp. (in Czech with an English summary).

Hybler, J. (1998) Polytypism of cronstedtite from Chvaletice and Litošice. *Ceramics-Silikáty*, **42**, 130–131.

Hybler, J., Petříček, V., Ďurovič, S. and Smrčok, L'. (2000) Refinement of the crystal structure of the cronstedtite-1*T*. *Clays and Clay Minerals*, **48**, 331–338.

International Tables for Crystallography, Volume A (1983) D. Reidel Publishing Company, Dordrecht, The Netherlands.

International Tables for X-ray Crystallography, Volume IV (1974) The Kynoch Press, Birmingham, England.

Kato, T. (1986) The crystal structure of yeatmanite. *Mineralogical Journal (Japan)* **13**, issue 2, 53–54.

Kogure, T., Hybler, J. and Ďurovič, S. (2001) A HRTEM study of cronstedtite: determination of polytypes and layer polarity in trioctahedral 1:1 phyllosilicates. *Clays and Clay Minerals*, **49**, 310–317.

Konnert, J.A., Appleman, D.E., Clark, J.R., Finger, L.W., Kato, T. and Miura, Y. (1976) Crystal structure and cation distribution of hulsite, a tin-iron borate. *American Mineralogist*, **61**, 116–122.

Ladd, M.F.C. and Palmer, R.A. (1977) *Structure Determination by X-ray Crystallography.* Plenum, New York, 393 pp.

Mellini, M. (1982) The crystal structure of lizardite-1*T*: hydrogen bonds and polytypism. *American Mineralogist*, **67**, 587–598.

Mellini, M. and Viti, C. (1994) Crystal structure of lizardite-1*T* from Elba, Italy. *American Mineralogist*, **79**, 1194–1198.

Mellini, M. and Zanazzi, P.F. (1987) Crystal structures of lizardite-1*T* and lizardite-2H_1 from Coli, Italy. *American Mineralogist*, **72**, 943–948.

Mellini, M., Weiss, Z., Rieder, M. and Drábek, M. (1996) Cs-ferrianite as a possible host of waste cesium. *European Journal of Mineralogy,* **8**, 1265–1271.

Mereiter, K. (1978) Die Kristallstruktur des Voltaits, $K_2Fe^{2+}_5Fe^{3+}_3Al(SO_4)_{12}{\cdot}18(H_2O)$ *Tschermaks Mineralogische*

und Petrographische Mitteilungen, **18**, 185–202.
Mikloš, D. (1975) Symmetry and polytypism of trioctahedral kaolin-type minerals. PhD thesis, Institute of Inorganic Chemistry, Slovak Academy of Sciences, Bratislava, Slovakia, 144 pp. (in Slovak).
Modaressi, A., Gerardin, R., Malaman, B. and Gleitzer, C. (1984) Structure et proprietes d'un germanate de fer de valence mixte $Fe_4Ge_2O_9$. Etude succinte de $Ge_xFe_{(3-x)}O4$ ($x < 0.5$). *Journal of Solid State Chemistry*, **53**, 22–24.
Palmer, D.C., Dove, M.T., Ibberson, R.M. and Powell, B.M. (1997) Structural behavior, crystal chemistry and phase transitions in substituted leucite: High resolution neutron powder diffraction studies. *American Mineralogist*, **82**, 16–29.
Petříček, V. and Dušek, M. (2000) *The crystallographic computing system JANA2000*. Institute of Physics, Praha, Czech Republic.
Radoslovich, E.W. (1961) Surface symmetry and cell dimension of layer-lattice silicates. *Nature, London*, **191**, 67–68.
Redhammer, G.J. (1998) Mössbauer spectroscopy and Rietveld refinement of synthetic ferri-Tschermak's molecule $CaFe^{3+}(Fe^{3+}Si)O_6$ substituted diopside. *European Journal of Mineralogy*, **10**, 439–452.
Renner, B. and Lehmann, G. (1986) Correlation of angular and bond length distortions in TO_4 units in crystals. *Zeitschrift für Kristallographie*, **175**, 43–59.
Robinson, K., Gibbs, G.V. and Ribbe, P.H. (1971) Quadratic elongation: A quantitative measure of distortion in coordination polyhedra. *Science*, **172**, 567–570.
Ross, C.R., Armbruster, T. and Canil, D. (1992) Crystal structure refinement of a spinelloid in the system Fe_3O_4-Fe_2SiO_4. *American Mineralogist*, **77**, 507–511.
Semenova, T.F., Rozhdestvenskaya, I.V. and Frank-Kamenetskii, V.A. (1977) Refinement of the crystal structure of tetraferri phlogopite. *Kristallografiya*, **22**, 1196–1201 (in Russian).
Smrčok, L'., Ďurovič, S., Petříček, V. and Weiss, Z. (1994) Refinement of the crystal structure of cronstedtite-3*T*. *Clays and Clay Minerals*, **42**, 544–551.
Steadman, R. (1964) The structure of trioctahedral kaolin-type silicates. *Acta Crystallographica*, **17**, 924–927.
Steadman, R. and Nuttall, P.M. (1963) Polymorphism in cronstedtite. *Acta Crystallographica*, **16**, 1–8.
Steadman, R. and Nuttall, P.M. (1964) Further polymorphism in cronstedtite. *Acta Crystallographica*, **17**, 404–406.
Steinfink, H. (1962) Crystal structure of a trioctahedral mica: Phlogopite. *American Mineralogist*, **47**, 886–889.
Tagai, T. and Joswig, W. (1985) Untersuchungen der Kationverteilung im Staurolith durch Neutronenbeugung bei 100 K . *Neues Jahbuch für Mineralogie Monatshefte*, 97–107.
Taylor, H.F.W. (1992) Tobermorite, jennite and cement gel. *Zeitschrift für Kristallographie*, **202**, 41–50.
Templeton, D.H. and Templeton, L.K. (1978) *Program AGNOST C*. University of California at Berkeley.
Toraya, H. (1981) Distortion of octahedra and octahedral sheets in 1*M* micas and the relation to their stability. *Zeitschrift für Kristallographie*, **157**, 173–190.
Wechsler, B.A., Lindsley, D.H. and Prewitt, C.T. (1984) The crystal structure and cation distribution in titanomagnetites ($Fe_{3-x}Ti_xO_4$). *American Mineralogist*, **69**, 754–770.
Weiss, Z., Rieder, M., Chmielová, M. and Krajíček, J. (1985) Geometry of the octahedral coordination in micas. *American Mineralogist*, **70**, 747–757.
Weiss, Z., Rieder, M. and Chmielová, M. (1992) Deformation of coordination polyhedra and their sheets in phyllosilicates. *European Journal of Mineralogy*, **4**, 665–682.
Wiewióra, A., Rausell-Colom, J.A. and García-Gonzáles, T. (1991) The structure of amesite from Mount Sobotka: A nonstandard polytype. *American Mineralogist*, **76**, 647–652.
Woodland, A.B. and Angel, R.J. (1998) Crystal structure of a new spinelloid with the wadsleyite structure in the system Fe_2SiO_4 – Fe_3O_4 and implications for the earth's mantle. *American Mineralogist*, **83**, 404–408.
Yakubovich, O.V., Simonov, M.A., Egorov-Tismenko, Y.K. and Belov, N.V. (1977) The crystal structure of a synthetic variety of alluadite. *Doklady Akademii Nauk SSSR*, **236**, 1123–1126 (in Russian).
Zheng, H. and Bailey, S.W. (1997) Refinement of an amesite-2H_1 polytype from Potmasburg, South Africa. *Clays and Clay Minerals*, **45**, 301–310.
Zhukhlistov, A.P. and Zvyagin, B.B. (1998) Crystal structure of lizardite-1*T* from electron diffractometry data. *Kristallographiya*, **43**, 1009–10014 (in Russian); also in: *Crystallography Reports* **43**, 950–955.

(*Received 25 June 2001; revised 6 March 2002; Ms. 560*)